Polymer, 1991, Vol. 32, 160–165

Electrical conductivity and optical properties of sensitized poly[(*N*-benzyldiphenylamino)-methane] with crystal violet

Panchanan Pramanik* and Md. Aquil Akhter
Department of Chemistry, Indian Institute of Technology, Kharagpur 721 302, India
(Received 9 May 1989; revised 1 January 1990; accepted 8 February 1990)

The dark conductivity and photoconductivity of poly[(*N*-benzyldiphenylamino)methane] was greatly enhanced in the dark and in the visible region by the addition of a small amount of crystal violet having a molar ratio of monomer:dopant from 1:0.007 to 1:0.03. The current–voltage characteristics were studied in the dark and in the visible wavelength range, and the current increased superlinearly with the increase of doping level. The activation energies for dark conductivity and photoconductivity are 0.73–0.64 eV and 0.71–0.60 eV, respectively, at different doping levels. The dye, crystal violet, introduced a new photoresponse maximum at 580 nm corresponding to the absorption spectrum of crystal violet.

(Keywords: poly[(*N*-benzyldiphenylamino)methane]; crystal violet; doping; conductivity; activation energy; space-charge-limited current; carrier)

INTRODUCTION

In continuation of our research[1–4] on photoconducting polymers, poly[(*N*-benzyldiphenylamino)methane] (PNBDM) was sensitized with the dye, crystal violet (CV), forming a photocurrent maximum corresponding to the absorption spectrum of crystal violet. The maximum photoresponse in the system PNBDM:CV was reached at a 1(monomer):0.03. The high photoresponse of this system in the visible region made it a good photoconductor. The synthesis and electrical and optoelectronic properties of PNBDM have been reported earlier[2]. The aim of the present paper is to report the investigations on PNBDM sensitized with CV. The detailed properties of PNBDM are mentioned elsewhere[2]. Its structure is shown in *Figure 1*.

EXPERIMENTAL

Crystal violet

Crystal violet (CV) was obtained from E. Merck AG, Darmstadt, Germany (C.I. no. 42555), having m.p. 215°C (dec.) and $\lambda_{max} = 588$ nm, and was purified further by crystallization from ethanol. Doped films were prepared (as reported earlier) by mixing dilute solutions of PNBDM and CV in chloroform, followed by pouring the mixture over a NESA† conducting laminated glass plate containing SnO_2 and allowing the solvent to evaporate[2,3]. The surface of the sandwich film configuration was found to be homogeneous by scanning electron microscopy and no crystallized aggregates were noticed. For undoped thin films the same procedure was adopted but in this case the mixing step was omitted. The relative molecular mass of the polymer is 2×10^4.

The steady-state dark conductivity and photoconductivity and spectral responses were investigated under vacuum (10^{-5} Torr) for samples possessing a sandwich configuration[2–5]. The conductivity measurements were made using a Keithly electrometer (610C, USA). The photocurrent was measured using a 600 W, 230 V tungsten–halogen lamp as a light source with an i.r. filter. The spectral response was measured using a high-intensity monochromator (CEL, HM104), a photon counter (CEL) and an electrometer, from which the normalized graph was obtained. The intensities at each wavelength were calibrated with a radiometer (CEL SM 204). The absorption spectra of the thin-film samples were investigated with a Carry-17-D spectrophotometer in the visible range.

RESULTS AND DISCUSSION

Current–voltage characteristics

The current–voltage characteristics of the sensitized samples were studied in the dark as well as under illuminated conditions (120 mW cm^{-2}). *Figure 2* shows a typical set of current–voltage characteristics for the different doping levels of the PNBDM:CV system. It is

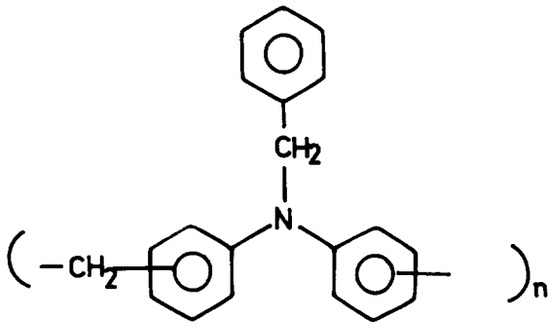

Figure 1 Structure of PNBDM

* To whom correspondence should be addressed

† Non-electrostatic shield formulation 'A'

0032-3861/91/010160-06

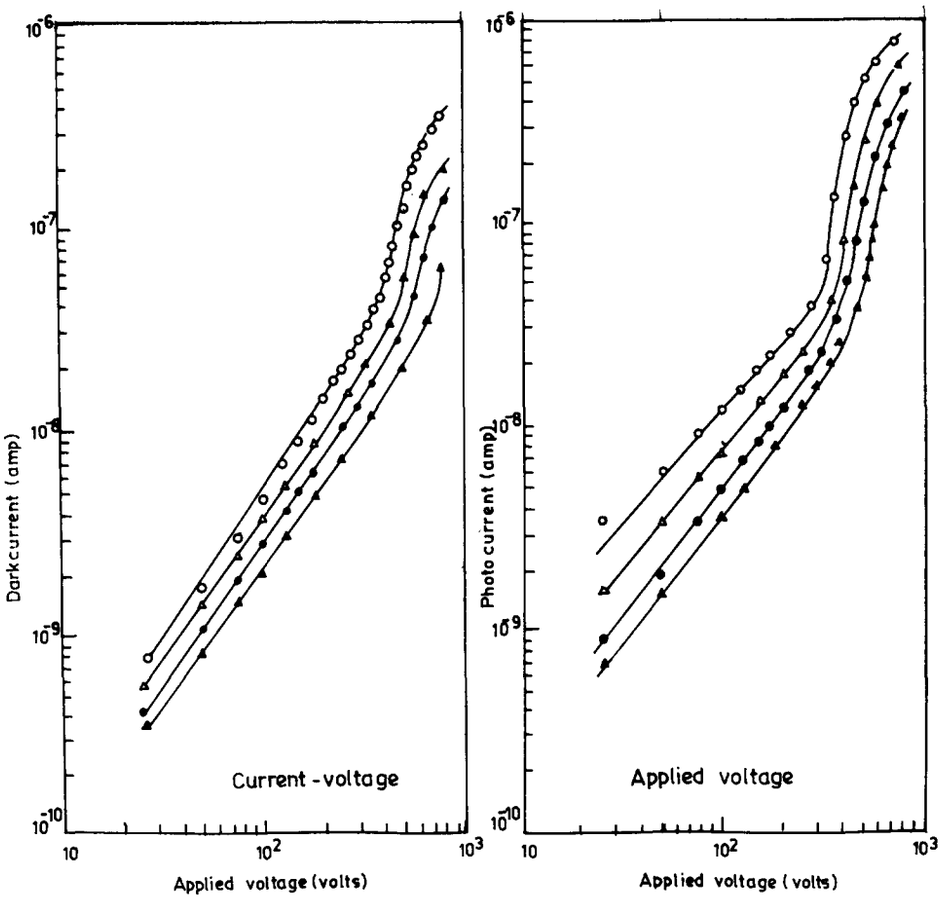

Figure 2 Dark current–voltage characteristics and photocurrent–voltage characteristics of PNBDM:CV: curve A (▲) 1:0.007; curve B (●) 1:0.009; curve C (△) 1:0.01; and curve D (○) 1:0.03. Thickness of film 20 μm and intensity of illumination 120 mW cm^{-2}

observed that the current–voltage curves are highly non-linear both in the dark and under illumination. When the current–voltage curves were plotted on log–log scale, some peculiar features were revealed. The current in the dark condition at low voltage increased gradually with the increase in bias voltage until it reached 400 V (thickness of the film 20 μm) at different concentrations of CV. On increasing the applied voltage above 400 V the current was found to increase rapidly by one order of magnitude within a very narrow range of bias voltage. After this transition, the current was found to increase only gradually with further increase of the voltage. Thus the current–voltage characteristics could be divided into three regions, viz. (i) the low-field region, (ii) the transition region and (iii) the high-field region. The transition and high field regions indicate that the current transport is space-charge-limited[6]. Above 400 V, i.e. case (ii), current–voltage characteristics can be explained by the shallow traps[7] due to the impurities, while above 600 V the same can be explained by the trap-filled-limit[8,9] current. The nature of the photocurrent–voltage plot as shown in *Figure 2* is almost similar to that for dark current–voltage plot, except that optical detrapping occurs at above 300 V instead of 400 V (in the dark). Thus, light has a greater effect on the current, and space-charge-limited current increases possibly due to effective detrapping by light. The photocurrent increases linearly below 300 V and then starts to increase super-linearly above 300 V. Thus the number of photocarriers increases with increasing applied voltage because the carriers that escape from recombination centres increase by lowering the potential energy barrier with increasing applied voltage. The doping level may introduce a greater effect on geminate-recombination phenomena under illumination, which enhances the superlinearity of the current–voltage curve.

Doping level in PNBDM

The dependence of the current on the doping level (expressed as mol% dopant per mole monomer) at a constant applied voltage 150 V and intensity of illumination 120 mW cm^{-2} is shown in *Figure 3*. It is noted that maximum response is attained when the molar ratio of monomer to CV is 1:0.03. As can be seen from *Figure 3*, the photocurrent increases faster at lower concentrations of CV in comparison to the dark current; this causes a sharp rise of the ratio of the photocurrent to dark current up to the concentration of CV of 0.01 mol%, after which this ratio becomes approximately constant. The current–voltage characteristics could be explained as follows. As the crystal violet concentration is increased from a low value, the photosensitivity increases probably due to increase of charge injection centres. But on further increase of CV dye concentration other processes, e.g. trapping, recombination, etc., are becoming dominant and the photosensitivity curve is almost linear. The rise and decay times observed for the sample having higher CV concentration could arise due to increased trapping of charge carriers in the PNBDM:CV system. The

current–voltage curves clearly show that the conduction process is non-ohmic in nature due to the presence of potential barriers at carrier generation centres or during the migration of carriers. The sudden rise of current in the transition region may be due to either the breakdown of barriers or the tunnelling of electrons through the trapping centres. The barrier height may reduce in the presence of light, which is noted in the investigations.

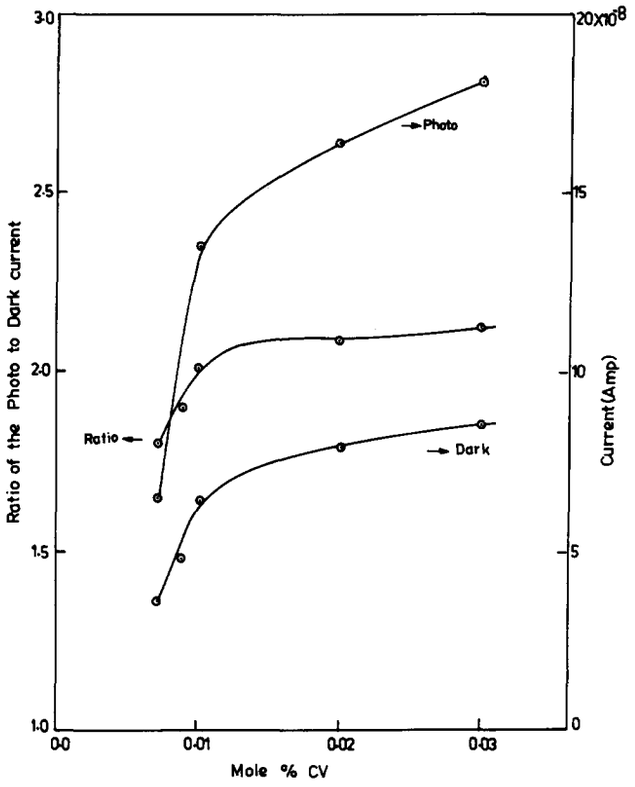

Figure 3 Ratio of photocurrent to dark current *versus* doping level in PNBDM:CV (film thickness 8 μm) at 300 K

Temperature dependence of conductivity

The temperature dependence of dark conductivity σ_d in the PNBDM:CV system is shown in *Figure 4*. The majority carriers appear to be electrons by the thermal probe method. The temperature dependence of photoconductivity σ_p in the PNBDM:CV system is shown in *Figure 4*. The relation between the dark conductivity and photoconductivity and the reciprocal of temperature in all the samples including pristine PNBDM obeyed the expressions $\sigma_d \propto \exp(-E_{ad}/kT)$ and $\sigma_p \propto \exp(-E_{ap}/kT)$, respectively. The activation energies[2] of dark conduction and photoconduction of pristine PNBDM were 1.16 and 1.05 eV, respectively, with electrons being the majority carriers. Starting from these values, the activation energies of dark conduction and photoconduction in sensitized PNBDM gradually decreased with the increase of CV content. *Figure 4* shows the log σ_d *versus* T^{-1} plots in the PNBDM:CV system. The apparent activation energies, E_{ad} and E_{ap}, obtained from *Figure 4* are shown in *Table 1*. In this system the activation energies gradually decrease with the increase of dopant content.

Activation energies were plotted against concentration of dopant, which is shown in *Figure 5*. The graph shows that activation energies of dark conduction and photoconduction decrease with increase of concentration of CV. The plots[10,11] of log σ_d and log σ_p against activation energies (*Figure 6*) show straight lines. Curves of dark conductivity and photoconductivity differ in slopes and intercepts:

$$\sigma_d = K \exp(-E_d/kT)$$
$$\sigma_p = K_1 \exp(-E_p/kT) \quad (1)$$

where K and K_1 are not equal and are independent of

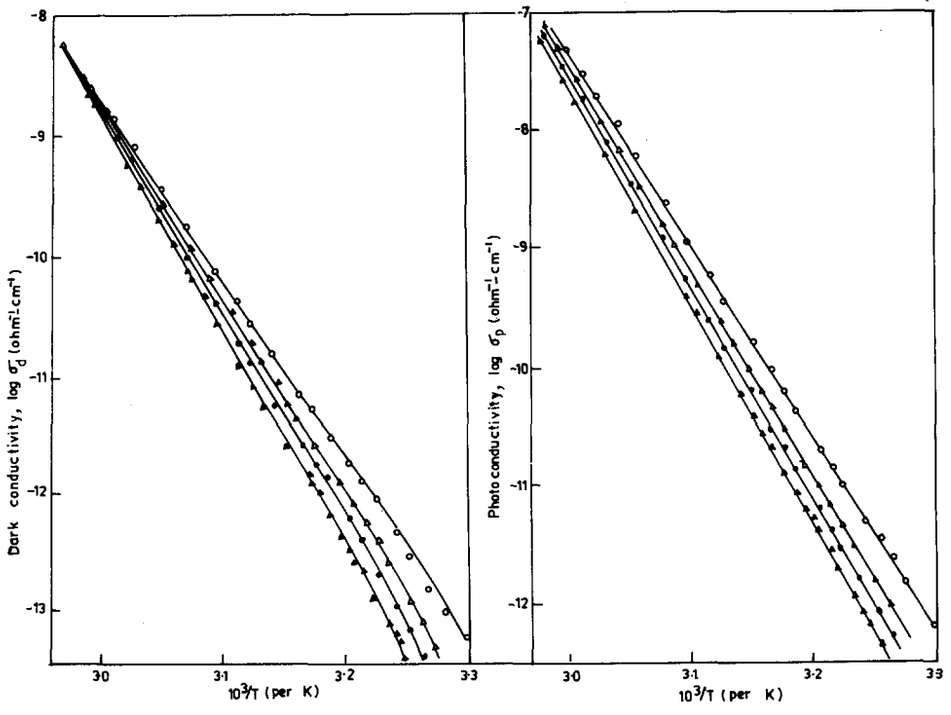

Figure 4 Dark conductivity and photoconductivity variation with temperature of PNBDM:CV. Film thickness 20 μm and intensity of illumination 120 mW cm^{-2}. Curves as in *Figure 2*

Table 1 Parameters obtained for various PNBDM:CV molar ratios

PNBDM:CV	Dark activation energy, E_{ad} (eV)	Photo activation energy, E_{ap} (eV)	Spectral peak at maximum (eV)
1:0	1.16	1.05	2.82
1:0.007	0.73	0.713	2.14 (580 nm)
1:0.009	0.71	0.69	2.14
1:0.01	0.68	0.63	2.14
1:0.03	0.64	0.60	2.14

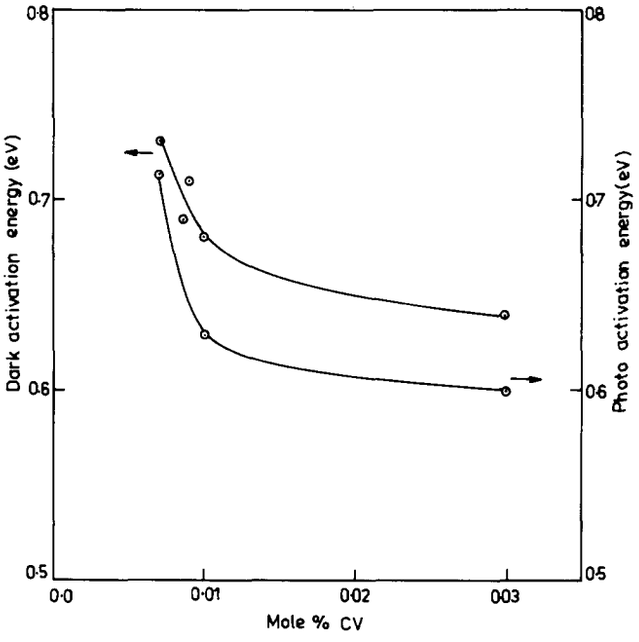

Figure 5 Activation energies plotted against dopant contents in PNBDM

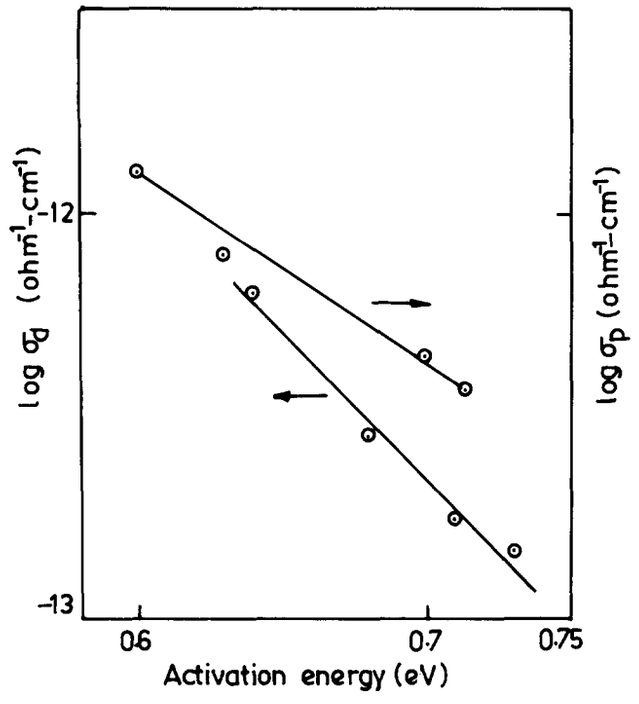

Figure 6 The relation between the conductivities at room temperature (300 K) and activation energies on PNBDM doped with different concentrations of CV

concentration of the CV dye. The constant values of K or K_1 observed for different concentrations of dye indicate that the mechanism of conduction is not changing with concentration of the dye (discussed also under 'Spectral properties').

Generally, there is a good correlation between conductivity and activation energy, or between carrier mobility and activation energy. This correlation can be expressed by an equation similar to an empirical equation applied to some polymers and amorphous silicon[12]. The probable explanation is that the charge carriers move by hopping between localized states in the polymer, which includes a large portion of amorphous regions. Then equation (1) turns out to mean that the dopants act to lower the activation energy for carrier hopping as K or K_1 remains independent of concentration of dye.

PNBDM has no apparent π-conjugated structure along the skeletal chains. The rate-determining step in carrier transport may be interchain or intrachain hopping.

Photocurrent kinetics

The promotion of electrons from shallow traps into the conducting state is a photo-detrapping process, which appears to control the photoconductivity. Photocurrent (I_p)–intensity (I) variation of PNBDM:CV film has been investigated for different doping levels. The photocurrent plotted against I on log–log scale as shown in *Figure 7* is linear. At low intensities of light[5,12] the photocurrent I_p varies with light intensity I as $I^{0.62}$, whereas at high light intensity, it is becoming saturated. The saturation of photoconductivity occurs when the intensity of light is greater than 120 mW cm^{-2}. The CV sensitizer has been shown to be the main source of the

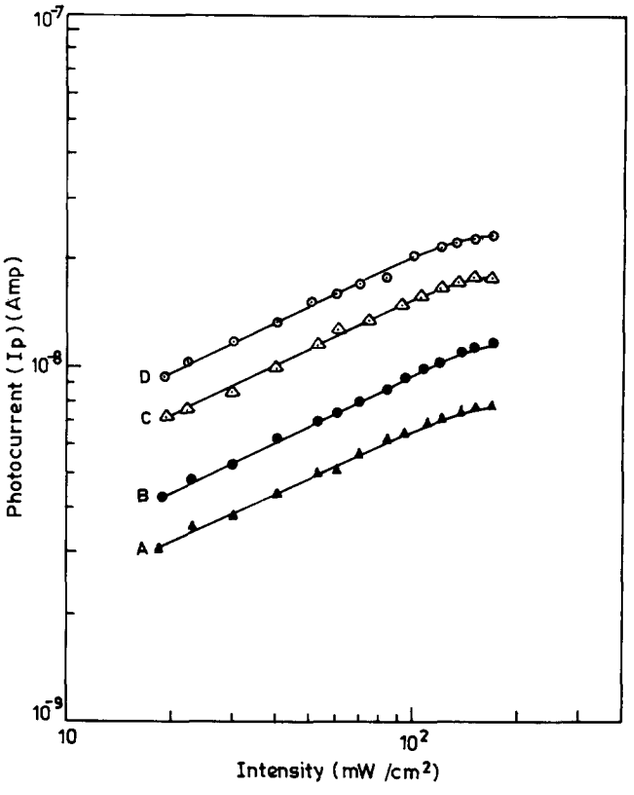

Figure 7 Photocurrent *versus* light intensity in PNBDM:CV (curves A–D as in *Figure 2*). Film thickness 20 μm and applied voltage 150 V at room temperature

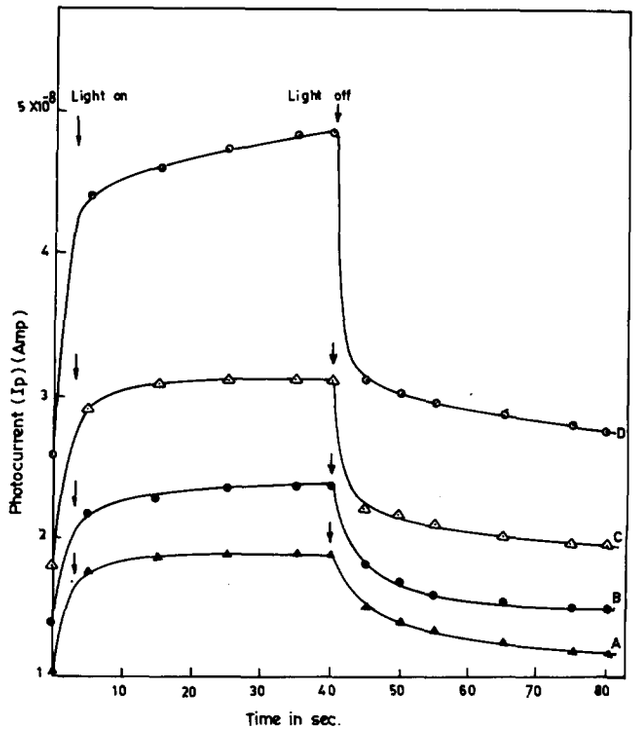

Figure 8 Rise and decay of photocurrent in PNBDM:CV (curves A–D as in *Figure 2*). Thickness of film 20 μm, intensity of illumination 120 mW cm^{-2} and applied voltage 300 V

photocarriers (*Figure 2*). The sensitizer also introduces a new set of traps and recombination centres having a range of energies that lie below the corresponding energies of PNBDM.

The rise and decay behaviours of the photocurrent for PNBDM:CV film with different dopant concentrations at room temperature are shown in *Figure 8*. It is noted that the rise and decay curves have become much slower with the increase of dopant concentration. This clearly indicates that, at higher CV concentration, more trapping centres of charge carriers have been introduced in the system.

Spectral properties

In this case the CV dye introduces a new photocurrent maximum at 580 nm corresponding to the absorption spectrum of CV. The absorption spectra of this dye in the polymer film at different concentrations are shown in *Figure 9*. *Figure 10* expresses the photocurrent action spectra of PNBDM with different concentration of CV in the usual way. At a very low concentration of CV a broad peak appears at 430 nm, which may correspond to pristine PNBDM[2]. The reduced sensitivity of the PNBDM:CV system may be attributed to inefficient transfer of exciton from dye to polymer or inefficient charge injection due to poor photoionization and to greater loss of carriers due to recombination and trapping. In discussing the mechanism of spectral sensitization, the following facts have been noticed, which are similar to those of other workers[12].

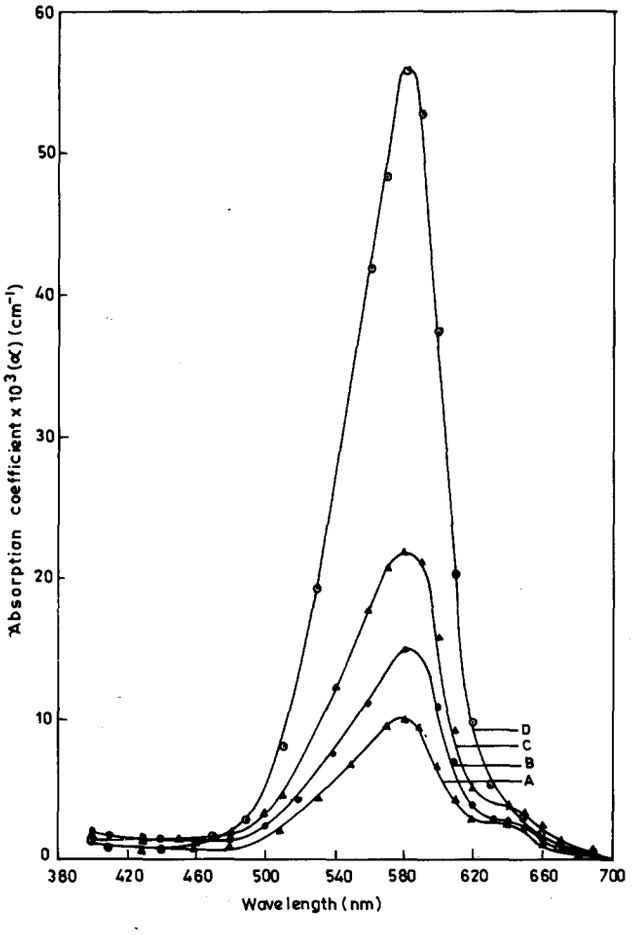

Figure 9 Absorption spectra of PNBDM:CV (curves A–D as in *Figure 2*) measured in film at room temperature (300 K)

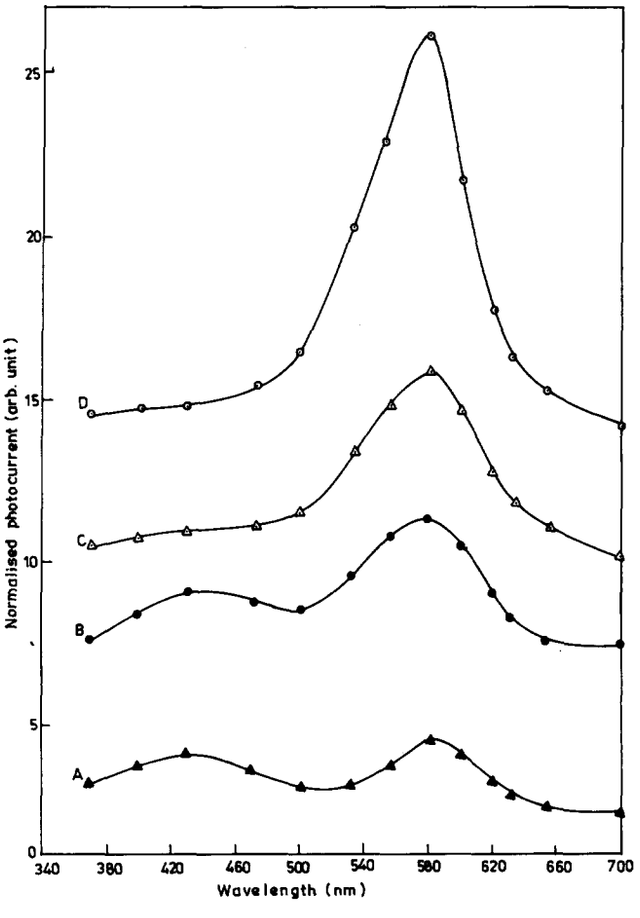

Figure 10 Spectral dependence of photocurrent in PNBDM:CV (curves A–D as in *Figure 2*). Thickness of film 20 μm

(a) The wavelength dependence of sensitized photoconductivity corresponds to the absorption spectrum of the dye. This indicates that the dye molecule is transferring its exciton to the polymer molecule and is causing some charge injection.

(b) The efficiency of dye sensitization depends upon the concentration of donor sites that may be formed by the monomer unit[13]. This donor site may be created by filling the excluded volume of the polymer with dye molecules.

It is now generally accepted that the sensitization process involves electron transfer between the excited state of the dye and the transporting polymer matrix[14]. The direction depends upon the relative energy levels of the dye and the polymer. Most systems transport holes more readily than electrons, so that electron transfer from the polymer to the excited dye is the situation usually encountered by the system. For hole transport the electron is injected into the highest occupied molecular orbital of the excited state of the dye. The separation of the resultant cation radical–anion radical pair is facilitated by an electric field applied to the photoconductor. For a system that transports electrons, the excited dye injects the electron into the lowest unoccupied molecular orbital of the polymer, which results in separation of cation radical–anion radical. The geminate-recombination rate of such pairs is lower, the higher the applied electric field (Onsager theory). The photogeneration efficiency is sometimes concentration-dependent. The dye molecules may also serve as a trap in the transport process in a dispersed system[15].

REFERENCES

1 Pramanik, P., Mukherjee, D. and Choudhary, T. K. *Ind. J. Chem.* (*A*) 1984, **23**(10), 839
2 Akhter, M. A., Pramanik, P. and Biswas, M. *J. Polym. Sci., Polym. Phys. Edn.* (*B*) 1987, **25**, 339
3 Pramanik, P. and Akhter, M. A. *Polymer* 1988, **29**, 746
4 Pramanik, P. and Akhter, M. A. *Polymer* 1988, **29**, 752
5 Kang, E. T., Ehrlich, P., Bhatt, A. P. and Anderson, W. A. *Macromolecules* 1984, **17**, 1020
6 Yun, M. S., Ozaki, M., Yoshino, K. and Inuishi, Y. *Japan. J. Appl. Phys.* 1983, **22**(12), 1810
7 Compos, M. *Mol. Cryst. Liq. Cryst.* 1972, **18**, 105
8 Helfrich, W. and Mark, P. *Z. Phys.* 1962, **168**, 495
9 Helfrich, W. and Mark, P. *Z. Phys.* 1962, **166**, 370
10 Kuroda, H., Kobayashi, M., Kinoshita, M. and Takemoto, S. *J. Chem. Phys.* 1962, **36**, 457
11 Tokito, J., Tsutsui, T. and Saito, S. *Polym. J.* 1985, **17**(8), 959
12 Kang, E. T., Ehrlich, P., Bhatt, A. P. and Anderson, W. A. *Appl. Phys. Lett.* 1982, **41**, 1136
13 Terreli, D. R. *Photogr. Sci. Eng.* 1977, **21**, 66
14 Gibson, H. W. *Polymer* 1984, **3**, 25
15 Mort, J. and Pfister, G. *Polym. Plast. Technol. Eng.* 1979, **12**(2), 89